Nano Energy 83 (2021) 105838

Contents lists available at ScienceDirect

Nano Energy

journal homepage: http://www.elsevier.com/locate/nanoen

Boron-modified cobalt iron layered double hydroxides for high efficiency seawater oxidation

Libo Wu [a,b], Luo Yu [a], Qiancheng Zhu [a], Brian McElhenny [a], Fanghao Zhang [a], Chunzheng Wu [c], Xinxin Xing [c], Jiming Bao [c], Shuo Chen [a], Zhifeng Ren [a,*]

[a] Department of Physics and Texas Center for Superconductivity at the University of Houston (TcSUH), University of Houston, Houston, TX 77204, USA
[b] Materials Science and Engineering Program, University of Houston, Houston, TX 77204, USA
[c] Department of Electrical and Computer Engineering, University of Houston, Houston, TX 77204, USA

ARTICLE INFO

Keywords:
Layered double hydroxide
Partially amorphous catalyst
Hierarchical structure
Oxygen evolution reaction
Seawater electrolysis

ABSTRACT

Developing efficient and stable oxygen evolution reaction (OER) catalysts that can work well at high current densities for seawater electrolysis is desirable but remains a significant challenge. Here a novel and scalable strategy is developed to synthesize partially amorphous boron-modified cobalt iron layered double hydroxides (B-Co_2Fe LDH). Benefiting from enhanced electronic kinetics and abundant active sites, this hierarchical nanosheet-nanoflake-structured B-Co_2Fe LDH catalyst shows superb OER catalytic activity, requiring overpotentials of 205 and 246 mV to drive current densities of 10 and 100 mA cm^{-2}, respectively, in 1 M KOH, along with a small Tafel slope of 39.2 mV dec^{-1}. Its partial amorphousness feature leads to enhanced stability and corrosion resistance, which help the B-Co_2Fe LDH catalyst to work well in the critical seawater condition. It requires overpotentials of 310 and 376 mV to drive current densities of 100 and 500 mA cm^{-2}, respectively, in 1 M KOH seawater and can work continuously for 100 h without producing any hypochlorite. This work can enable the development of LDH catalysts for highly selective seawater oxidation using a general approach.

1. Introduction

Water electrolysis to produce high caloric hydrogen is a sustainable and environmentally friendly energy-conversion technology that can be used to decrease the excessive consumption of fossil fuels [1,2]. In general, water electrolysis comprises two redox reactions: the cathodic hydrogen evolution reaction (HER) and the anodic oxygen evolution reaction (OER), of which OER is kinetically slower and controls the overall efficiency [3–5]. To make overall water electrolysis more energy-efficient and cost-effective, catalytically active OER catalysts with long-term stability are in significant demand. On the other hand, most current electrocatalytic research focuses on the splitting of fresh water, which is a scarce resource in many regions around the world [6,7]. Seawater, representing more than 96% of Earth's total water reserves, is an unlimited resource and has great potential for hydrogen generation [8,9]. It is also easier to combine seawater electrolysis with the sustainable electricity-generation technologies (such as wave, solar, and wind) employed in the coastal zones [10,11]. Moreover, the consumption of H_2 and O_2 gas produced by seawater electrolysis can produce safe drinking water, which is very meaningful for the coastal arid areas [8,12,13]. Compared with freshwater electrolysis, seawater electrolysis is more challenging due to the existence of chloride anions (Cl^-, ~ 0.5 M), which will compete with OER and form hypochlorite (ClO^-) at high oxidation potential [6]. Compared with acid or neutral electrolytes, an alkaline electrolyte can provide a larger overpotential (η) limit for selective OER. Under an alkaline condition (pH > 7.5), the theoretical voltage for hypochlorite formation in seawater ($Cl^- + 2OH = ClO^- + H_2O + 2e^-$) is around 480 mV higher than that of OER [6,7]. That is to say, an OER catalyst must work at an overpotential lower than 480 mV for 100% seawater oxidation. Other critical issues in seawater electrolysis are chloride corrosion and the presence of insoluble precipitations [any of $Ca(OH)_2$/$Mg(OH)_2$, dust, or microbes], both of which will result in the corrosion or poisoning of the catalyst and the decay of its catalytic performance [10,12,13].

Among all of the catalysts studied for alkaline freshwater oxidation, layered double hydroxides (LDHs) are the most promising due to their high intrinsic OER activity and tunable chemical composition feature [14,15]. Ni-Fe LDH was reported as an advanced OER catalyst by Gong

* Corresponding author.
E-mail address: zren@uh.edu (Z. Ren).

https://doi.org/10.1016/j.nanoen.2021.105838
Received 30 November 2020; Received in revised form 19 January 2021; Accepted 28 January 2021
Available online 30 January 2021
2211-2855/Published by Elsevier Ltd.

et al. in 2013 and tremendous bi- and trimetallic LDHs, as well as their compositions, have been explored and demonstrated to be efficient OER catalysts [4,16–26]. However, LDH-based catalysts still suffer from deficiencies like poor electronic conductivity and limited active sites, which need further enhancement for their application in industrial hydrogen production [25,27]. Constructing self-supported LDH-based catalysts on conductive substrates like nickel foam [4,17,23], copper foam [18,21], and carbon cloth [22] is an effective way to enhance their conductivity and stability but is still not adequate. Another issue is that hydrothermal reaction, the most used synthesis method for LDH-based catalysts, commonly requires strict reaction conditions (maintenance at temperatures above the boiling point of water for 6–12 h in a sealed container) that are not suitable for scaling up and always lead to a nanosheet structure [15]. An easily scalable synthesis method, as well as a novel structure that can rivet and expose more active sites to enhance the catalytic activity should be explored to promote the potential practical application of the LDH catalysts. Very recently, amorphous catalysts have been greeted with great enthusiasm due to their structural and chemical advantages [28–31]. Normally, amorphous catalysts possess a large number of percolation pathways and a fast ion-diffusion feature due to their structure disorder and relatively loose packing of atoms [28,32–36]. Among various amorphous catalysts, boron-based ones such as Co_2B [29], Fe-Ni-P-B-O [30], Gd-CoB@Au [37], and $Cr_{1-x}Mo_xB_2$ [38] have recently been synthesized and shown to exhibit high catalytic activity [39–42].

Considering the features of LDH- and amorphous boron-based catalysts, amorphous boron-modified LDH materials might be promising catalysts for seawater electrolysis, although relevant studies remain quite limited [6,10,43]. Here, for the first time, we synthesized partially amorphous boron-modified cobalt iron layered double hydroxides (denoted as B-Co_2Fe LDH) using a two-step water bath reaction-chemical reduction approach in an open beaker at low temperature. A unique hierarchical nanosheet-nanoflake structure was obtained by tuning the Co/Fe ratio in the reactants and the partial amorphousness feature was then achieved by the boron modification. The catalyst's open and hierarchical architecture, along with the partial amorphousness feature, allows for abundant active sites, enhanced electronic kinetics, and high corrosion resistance. Typically, it requires overpotentials of only 205 and 246 mV to drive current densities of 10 and 100 mA cm^{-2}, respectively, in 1 M KOH and it exhibits a small Tafel slope of 39.2 mV dec^{-1}, which place it among the best self-supported OER catalysts reported thus far. As for seawater oxidation, it requires overpotentials of 310 and 376 mV to drive current densities of 100 and 500 mA cm^{-2}, respectively, in 1 M KOH seawater and can work continuously for 100 h without producing any hypochlorite. in situ and *ex situ* Raman tests and post-OER analysis were applied to reveal its transformation during OER. Long-term immersion and corrosion testing, as well as chronopotentiometric measurements, were applied to prove its corrosion resistance and catalytic durability.

2. Results and discussion

As illustrated in Fig. 1a, a two-step water bath reaction-chemical reduction procedure was applied to synthesize partially amorphous B-Co_2Fe LDH. Here, commercial nickel foam (NF) was employed as the substrate due to its three-dimensional structure, high conductivity, and

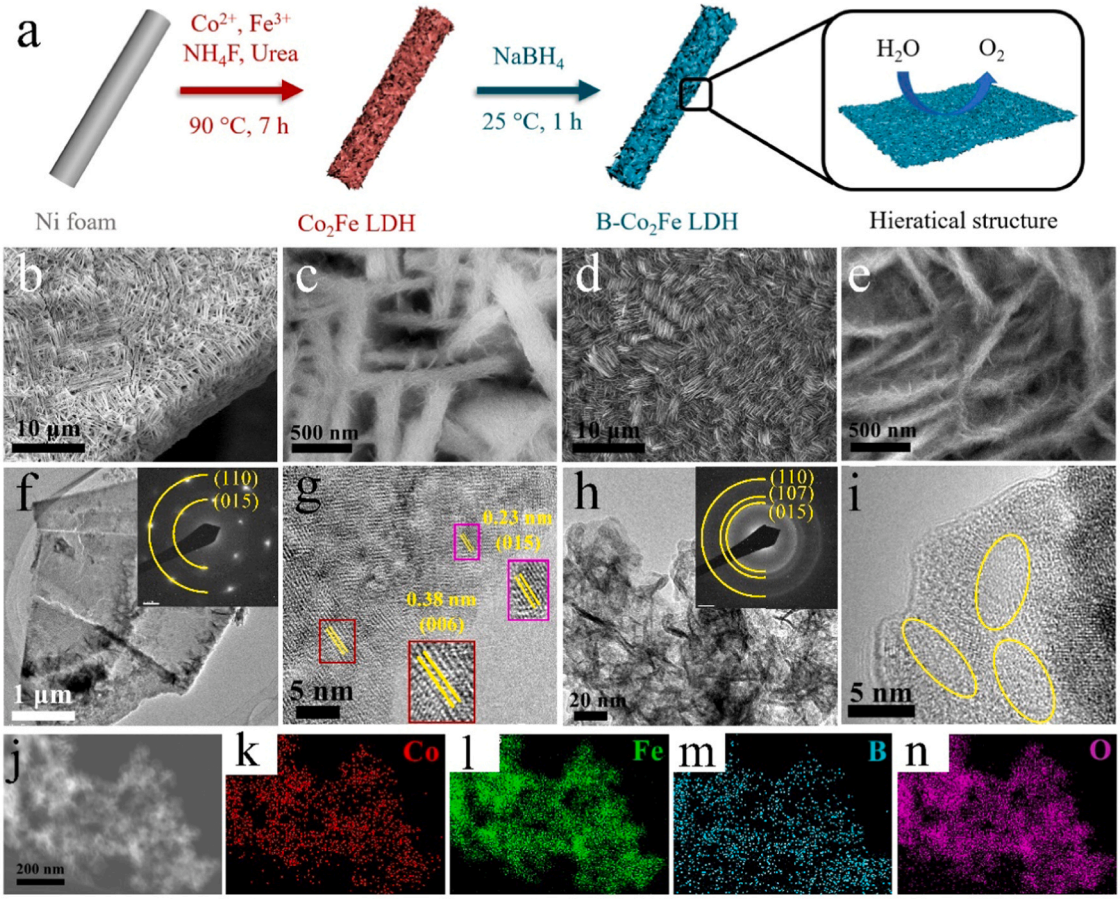

Fig. 1. (a) Schematic illustration of the formation of partially amorphous B-Co_2Fe LDH via a two-step water bath reaction-chemical reduction procedure. (b-c) SEM, (f) TEM, and (g) HRTEM images of the Co_2Fe LDH precursor. Inset to (f): SAED pattern. (d-e) SEM, (h) TEM, and (i) HRTEM images of partially amorphous B-Co_2Fe LDH. Inset to (h): SAED pattern. (j) TEM image of partially amorphous B-Co_2Fe LDH and the corresponding EDX element mapping for (k) Co, (l) Fe, (m) B, and (n) O.

low cost [44]. Scanning electron microscopy (SEM) images show that the structure of the Co_xFe_y LDH(x/y = 3/1, 2/1, 1/1, and 1/2) precursors could be tuned from nanorods (Co_3Fe LDH in Fig. S1, Supporting Information) to nanosheets with numerous nanoflakes attached on the surface (Co_2Fe LDH in Figs. S2 and 1b–c, and CoFe LDH in Fig. S3) and finally transformed to dense nanosheets stacked together ($CoFe_2$ LDH in Fig. S4) by adjusting the Co/Fe ratio in the initial reactants. Meanwhile, $Co(OH)_2$ (Fig. S5) and $Fe_6(OH)_{12}CO_3.2\,H_2O$ (Fe CH) (Fig. S6) precursors exhibit nanoflake and nanosheet structures, respectively. The Co_2Fe LDH precursor, which has a hierarchical nanosheet-nanoflake architecture and superior OER catalytic activity compared with others (Fig. S7), was then selected to prepare the partially amorphous boron-modified Co_2Fe LDH catalyst.

In the subsequent chemical reduction step, a series of B-Co_2Fe LDH-Z (Z = 0.25, 0.5, 1, and 2) samples were obtained by soaking Co_2Fe LDH precursors in 0.25, 0.5, 1, and 2 M $NaBH_4$ solution, respectively, at room temperature for 1 h. The H^-, which originates from $NaBH_4$ and exhibits strong reducing ability, can act as an oxygen scavenger to create oxygen defects and modify the crystallinity of the precursor [32,45]. As shown in Fig. S8-11 and Fig. 1d–e, these B-Co_2Fe LDH samples share a thinner nanosheet and more porous nanoflake structure compared with the Co_2Fe LDH precursor. Such hierarchical structure can dramatically enhance the surface area to disperse and expose more active sites for water electrolysis compared with the pure nanosheet structure [15,25]. The SEM images of B-$Co(OH)_2$ and B-Fe CH shown in Fig. S12-13, respectively, also confirm that their structures could be slightly tuned through modification by the $NaBH_4$ solution. Among all of these B-Co_2Fe LDH-Z samples, the one modified by 0.5 M $NaBH_4$ solution was found to exhibit the best OER activity (Fig. S14) and was selected as the representative sample, specifically denoted as B-Co_2Fe LDH in the following discussion. This self-supported B-Co_2Fe LDH catalyst exhibits a hydrophilic feature, as demonstrated in Video S1, showing a sharp contrast with the pristine NF, which exhibits a hydrophobic feature. Recent studies have confirmed that a hydrophilic surface feature is generally helpful for fast electrolyte diffusion and easier gas bubble release during water electrolysis [12,46,47].

doi:10.1016/j.nanoen.2021.105838

Transmission electron microscopy (TEM) analysis was then performed to characterize the structures in detail. As shown in Fig. 1f, a slice of almost transparent Co_2Fe LDH precursor nanosheet with numerous nanoflakes on its edges can be clearly observed. The interplanar spacings in the high-resolution TEM (HRTEM) image in Fig. 1g were measured to be 0.38 and 0.23 nm, corresponding to the (006) and (015) planes of Co_2Fe LDH, respectively. Additionally, the discrete dots in the selected area electron diffraction (SAED) pattern shown in the inset to Fig. 1f reveal the characteristic (015) and (110) facets of Co_2Fe LDH. The clear space fringes along with the sharp discrete dots indicate that the Co_2Fe LDH precursor has a crystalline structure. On the other hand, the TEM image of B-Co_2Fe LDH in Fig. 1h shows a more porous structure and the detailed HRTEM image in Fig. 1i indicates that parts of the sample are amorphous (marked by yellow ellipses), which is further confirmed by the broad rings, normally recognized as the intrinsic characteristic of an amorphous material [30,48], in the SAED pattern shown in the inset to Fig. 1h. The uniform modification of boron inside a single B-Co_2Fe LDH nanosheet (Fig. 1j) is illustrated by the energy-dispersive X-ray spectrometry (EDX) mapping images in Fig. 1k–n.

The exact phase compositions and crystal structures of these samples were detected by X-ray diffraction (XRD). The resulting curve for the Co_2Fe LDH precursor in Fig. 2a corresponds well to cobalt iron carbonate hydroxide (JCPDS#50–0235), showing that the LDH material can be successfully synthesized by this low-temperature water-bath

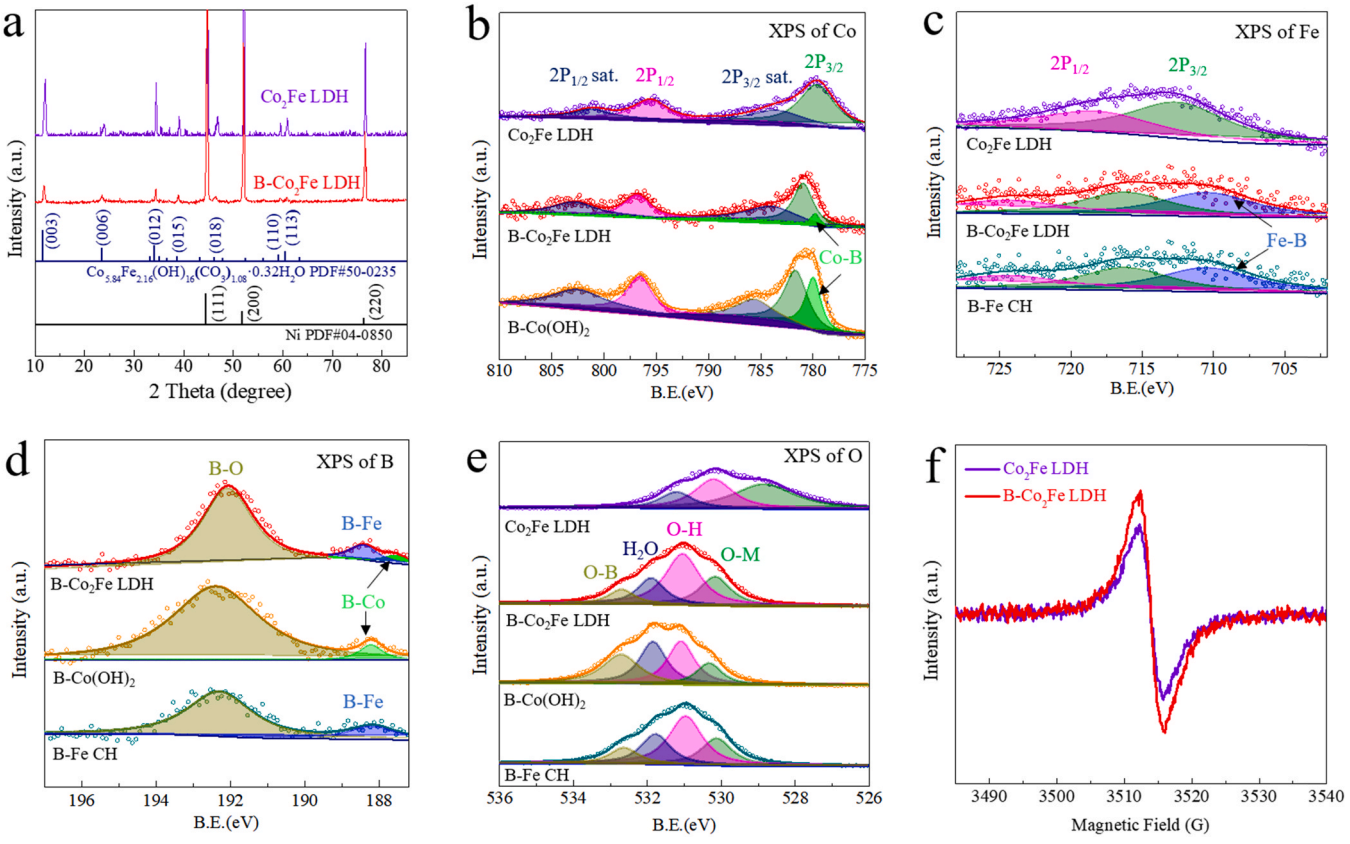

Fig. 2. (a) XRD patterns of the Co_2Fe LDH precursor and B-Co_2Fe LDH along with the standard PDF cards for cobalt iron carbonate hydroxide (JCPDS#50–0235) and Ni (JCPDS#04–0850). High-resolution XPS spectra of (b) Co, (c) Fe, (d) B, and (e) O for the as-prepared catalysts. (f) EPR spectra of Co_2Fe LDH and B-Co_2Fe LDH catalysts.

reaction. Compared with that of the Co_2Fe LDH precursor, the lower intensity and broader half-width of the main diffraction peaks in the B-Co_2Fe LDH curve indicates that the modification by boron can decrease the crystallinity [31,37,49]. This phenomenon can also be observed in the XRD patterns of B-$Co(OH)_2$ and B-Fe CH samples (Fig. S15a–b, respectively), in which the intensity of the main peaks for the boron-modified samples is lower than that for the initial precursors. A similar phenomenon, that the $NaBH_4$ solution can lower the crystallinity of the material being modified or even transform it to completely amorphous, has been previously reported [31,32,37,43,49]. To investigate the change of the valence states before and after the boron-modification, X-ray photoelectron spectroscopy (XPS) was conducted. As shown in Fig. 2b, in addition to a pair of satellite peaks, the high-resolution XPS spectra of Co 2p for the Co_2Fe LDH precursor can be deconvolved to a Co^{2+} $2p_{3/2}$ peak at 781.3 eV and a Co^{2+} $2p_{1/2}$ peak at 796.7 eV [26]. An additional peak for Co-B at 778.0 eV can be observed in both B-Co_2Fe LDH and B-$Co(OH)_2$, suggesting that the modification by boron could lead to the formation of a Co-B bond [29]. Similarly, a peak for Fe-B at 707.4 eV can be observed in the high-resolution XPS spectra of Fe for both the B-Co_2Fe LDH and B-Fe CH samples, in addition to the regular Fe^{3+} $2p_{3/2}$ and $2p_{1/2}$ peaks (Fig. 2c). Both Co and Fe were positively shifted to higher oxidation states by the boron modification. As for the XPS spectra of B (Fig. 2d), in addition to the huge oxidation peak for B-O at 192.0 eV, peaks for B-Co at 188.1 eV and B-Fe at 187.9 eV can be found in B-Co_2Fe LDH [49]. These XPS results prove that the $NaBH_4$ solution can not only tune the structure and phase of Co_2Fe LDH, but can also react with it to form metallic boride [30]. As for the XPS spectra of O in Fig. 2e, the peaks located at 529.3, 531.1, and 532.8 eV are assigned to oxygen-metal (O-M), hydroxide (O-H), and chemisorbed water on the surface (H_2O), respectively [22,33]. Additionally, an extra peak for O-B located at 533 eV can be found for each of the boron-modified catalysts. The asymmetric nature of the high energy hydroxide bond (O-H) in the XPS spectrum indicates the presence of oxygen vacancies, so the relative peak area ratio of O-H/O-M can be used to roughly assess the amount of oxygen defects [33,50,51]. Fig. 2e clearly shows that the ratio of O-H/O-M in the B-Co_2Fe LDH is higher than that of the pristine Co_2Fe LDH precursor, confirming relatively more oxygen defects. Additionally, the stronger magnetic signal at around 3514 G for the B-Co_2Fe LDH catalyst, determined by electron paramagnetic resonance (EPR) spectroscopy (Fig. 2f) indicates a higher concentration of unpaired electrons, which generally results from oxygen defects [32,52]. Thus, both XPS and EPR data prove that more oxygen defects were created by boron modification.

The OER activity of these catalysts was evaluated in three types of electrolytes (1 M KOH, 1 M KOH + 0.5 M NaCl, and 1 M KOH seawater), respectively. To avoid the oxidation peak and precisely measure the overpotential at small current density, all polarization curves for these catalysts were collected from high to low potential with a scan rate of 2 mV s^{-1}. As shown in Fig. 3a, the optimal partially amorphous B-Co_2Fe LDH catalyst requires overpotentials of only 205, 246, 289, and 309 mV to attain current densities of 10, 100, 500, and 1000 mA cm^{-2}, respectively, in 1 M KOH, superior to that of boron-modified single-metallic hydroxide catalysts [B-$Co(OH)_2$ and B-Fe CH], the pristine bimetallic LDH catalyst (Co_2Fe LDH), and the benchmark noble-metal-based catalyst (IrO_2). The catalytic performance of the B-Co_2Fe LDH catalyst in 1 M KOH is also directly verified by Video S2, in which vigorous O_2 bubbles release from the surface instantly and no peeled-off catalyst can be observed, demonstrating excellent structure stability at high current densities. The Tafel slope value of partially amorphous B-Co_2Fe LDH is only 39.2 mV dec^{-1} (Fig. 3b), which is the lowest among all of these catalysts and indicates a higher transfer coefficient and enhanced electrocatalytic kinetics. Such low overpotentials (η_{10} = 205 mV and η_{100} = 246 mV, where η_{10} and η_{100} are the overpotentials required to achieve current densities of 10 and 100 mA cm^{-2}, respectively) together with a small Tafel slope (39.2 mV dec^{-1}) place the B-Co_2Fe LDH catalyst among the best documented self-supported catalysts reported thus far (Table S1). The modification by boron can significantly enhance the conductivity of these catalysts as revealed by the electrochemical impedance spectroscopy (EIS) analysis in Fig. 3**c**. Based on the equivalent circuit (inset, Fig. 3c), the charge-transfer resistance (R_{ct}) values of

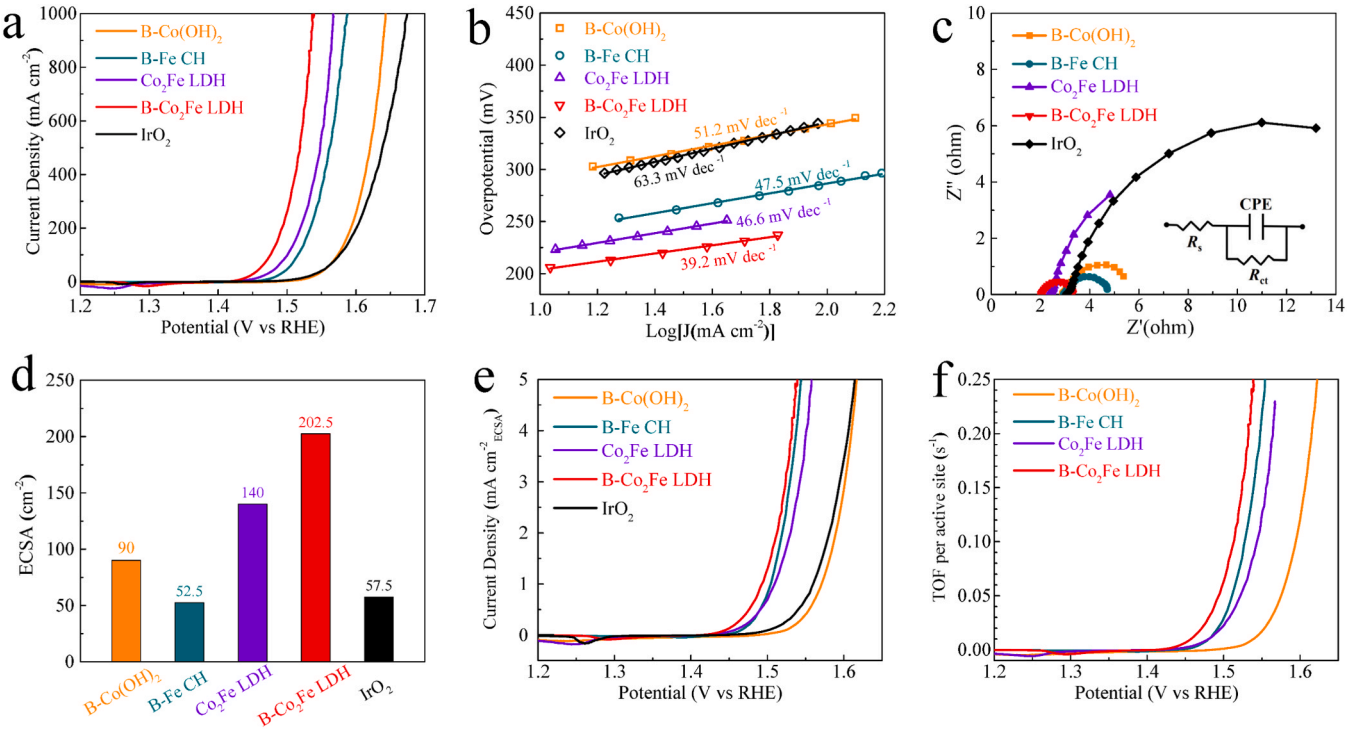

Fig. 3. (a) OER polarization curves of B-$Co(OH)_2$, B-Fe CH, Co_2Fe LDH, B-Co_2Fe LDH, and IrO_2 catalysts in 1 M KOH electrolyte. (b) Tafel plots derived from the polarization curves in (a). (c) Nyquist plots, (d) ECSA, and (e) ECSA-normalized OER activity of these catalysts. (f) TOF curves of the B-$Co(OH)_2$, B-Fe CH, Co_2Fe LDH, and B-Co_2Fe LDH catalysts.

partially amorphous B-Co_2Fe LDH, B-$Co(OH)_2$, and B-–Fe CH were measured to be ~ 1.3, ~ 3.0, and ~1.9 Ω, respectively, much smaller than those of the Co_2Fe LDH precursor (~ 11.7 Ω) and IrO_2 (~ 16.4 Ω). Such an enhancement of conductivity for these boron-modified catalysts should be attributed to the morphology tuning and the formation of conductive metallic boride on their surfaces. The electrochemically active surface area (ECSA) of each catalyst, which is proportional to its double-layer capacitance (C_{dl}) shown in Fig. S16, can be used to evaluate the catalyst's intrinsic surface-area activity. As shown in Fig. 3d, the ECSA of B-Co_2Fe LDH (202.5 cm^{-2}_{ECSA}) is larger than that of the Co_2Fe LDH precursor (140 cm^{-2}_{ECSA}), which is due to the greater number of oxygen defects and the partial amorphousness feature created through the modification by boron. We further normalized current density by the ECSA (Fig. 3e) and the partially amorphous B-Co_2Fe LDH catalyst still exhibited the best OER activity, indicating its highest intrinsic catalytic activity among these catalysts. Furthermore, the turnover frequency (TOF) value of the B-Co_2Fe LDH catalyst at the potential of 1.50 V vs. RHE ($\eta = 270$ mV) is calculated to be 0.065 s^{-1} (Fig. 3f), which is much higher than that of B-$Co(OH)_2$ (0.0089 s^{-1}), B-Fe CH (0.026 s^{-1}), and the pristine Co_2Fe LDH precursor (0.023 s^{-1}), indicating its highest instantaneous efficiency for OER.

doi:10.1016/j.nanoen.2021.105838

As mentioned above, the most critical challenge for alkaline seawater electrolysis is the formation of hypochlorite, which will compete with OER and severely lower the efficiency of seawater oxidation. This B-Co_2Fe LDH catalyst requires an overpotential of 309 mV to drive a large current density of 1000 mA cm^{-2} in 1 M KOH, much lower than the maximum theoretical value of ~ 480 mV for avoiding the formation of hypochlorite. Its corrosion resistance performance in natural seawater was first roughly evaluated using long-term immersion testing. As shown in Fig. S17, no obvious corrosion pitting or structural collapse can be found at different magnification levels after immersion in natural seawater for 28 days, indicating excellent structure stability. We then conducted corrosion testing of Co_2Fe LDH and B-Co_2Fe LDH catalysts in natural seawater, and the corresponding data are displayed in Fig. S18 and Fig. 4a. The corrosion current density of B-Co_2Fe LDH is merely 1.38 μA cm^{-2}, which is around half of that of Co_2Fe LDH (2.4 μA cm^{-2}), showing its higher corrosion resistance after boron modification. The excellent structure stability and the high corrosion resistance indicate that this partially amorphous B-Co_2Fe LDH has a high probability to be a stable catalyst for seawater oxidation. We then measured the OER activity of all of these as-prepared catalysts in both alkaline saline (1 M KOH in 0.5 M NaCl water, simulated seawater electrolyte) and alkaline seawater (1 M KOH seawater). As shown in Fig. S19a, all five catalysts show a slight decline in OER activity when tested in alkaline saline water than in pure water due to the blockage of active sites by the Cl^-. This

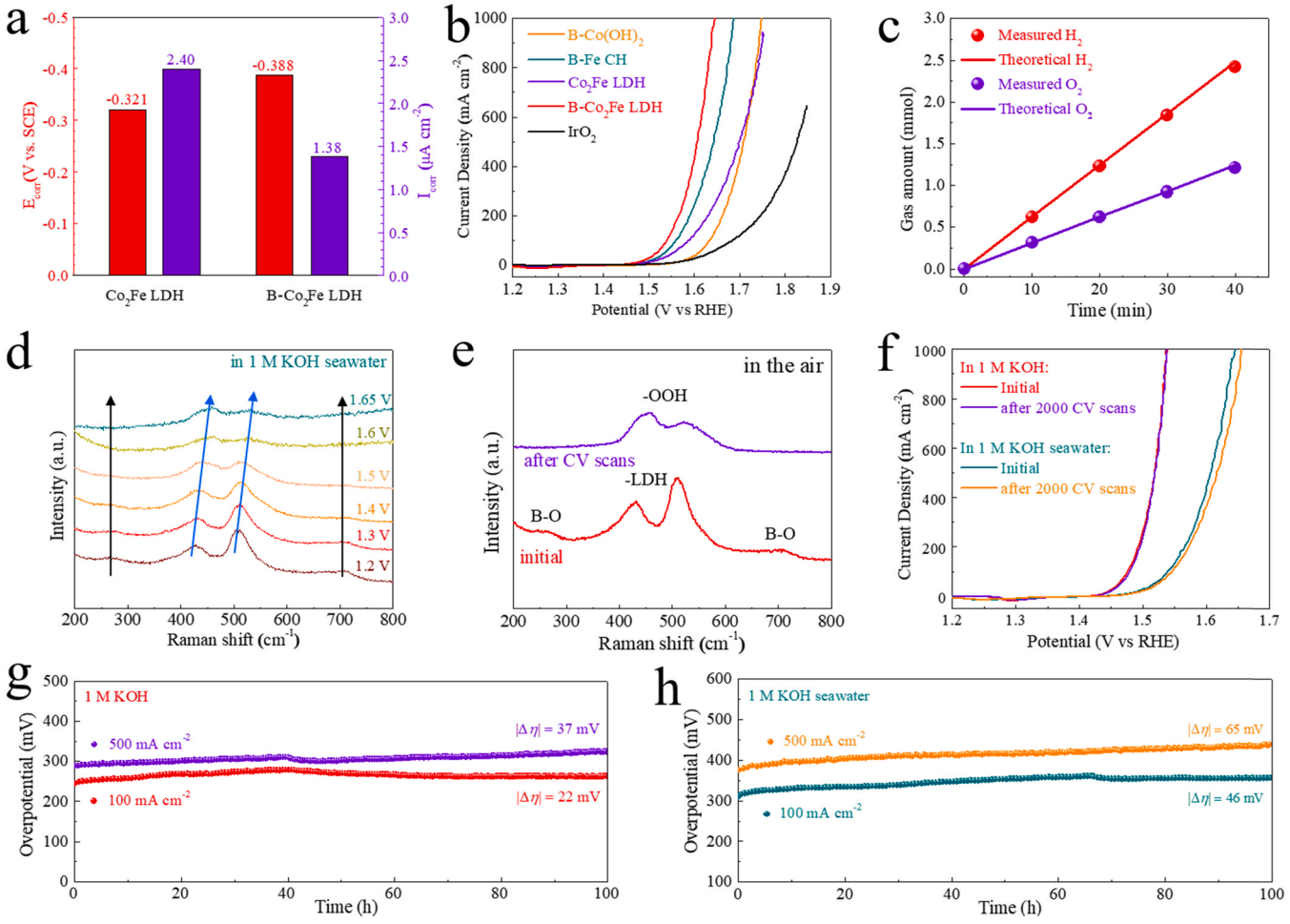

Fig. 4. (a) Corrosion potentials (red) and corrosion current densities (purple) of Co_2Fe LDH and B-Co_2Fe LDH catalysts in natural seawater. (b) OER polarization curves of the B-$Co(OH)_2$, B-Fe CH, Co_2Fe LDH, B-Co_2Fe LDH, and IrO_2 catalysts in 1 M KOH seawater electrolyte. (c) Measured (dots) and theoretical (solid lines) gaseous products from B-Co_2Fe LDH at a current density of 500 mA cm^{-2} in 1 M KOH seawater. (d) in situ Raman spectra of B-Co_2Fe LDH running from 1.2 to 1.65 V (V vs. RHE) in 1 M KOH seawater. (e) *ex situ* Raman spectra of B-Co_2Fe LDH before and after 100 CV scans in 1 M KOH seawater in the air. (f) OER polarization curves of B-Co_2Fe LDH before and after 2000 CV scans in 1 M KOH and 1 M KOH seawater. Chronopotentiometric curves of B-Co_2Fe LDH at constant current densities of 100 and 500 mA cm^{-2} in (g) 1 M KOH and (h) 1 M KOH seawater electrolytes.

decline was greatly increased when the catalysts were tested under the actual seawater condition (Fig. 4b), which has a much more complicated composition, such as including alkaline metal cations (Ca^{2+}, Mg^{2+}, Na^{+}, K^{+}) chloride ions (Cl^{-}), sulfate ions (SO_2^{4-}), and insoluble precipitates. Specifically, the B-Co_2Fe LDH catalyst requires overpotentials of 245, 310, 376, and 415 mV to drive current densities of 10, 100, 500, and 1000 mA cm^{-2}, respectively, in 1 M KOH seawater. The Tafel slope values of these catalysts in different electrolytes shown in Fig. S19b–d also indicate that their catalytic kinetics and transfer coefficient values are slightly and severely lowered in saline and natural seawater, respectively. The catalytic performance of the B-Co_2Fe LDH catalyst in 1 M KOH seawater is verified by Video S3, in which this catalyst is observed to work effectively to produce oxygen gas at low and high current densities in the turbid electrolyte. Even though the Co_2Fe LDH precursor shows the second-best OER activity among these catalysts in 1 M KOH (Fig. 3a), its performance declined more heavily than that of the boron-modified ones when tested in alkaline seawater (Fig. 4b). This proves that the modification by boron, which can enhance a catalyst's conductivity and enlarge its ECSA, contributes significantly to maintaining catalytic activity in the critical seawater electrolyte. The faradaic efficiency of B-Co_2Fe LDH was measured by a gas chromatography (GC) test performed at a current density of 500 mA cm^{-2} in 1 M KOH seawater to identify whether this catalyst can work efficiently for seawater oxidation. As shown in Fig. 4c, the amount of measured O_2 gas matches well with the theoretical values, showing a faradaic efficiency higher than 97.5%. in situ Raman testing was then performed to reveal the transformation of this catalyst during OER. As shown in Fig. 4d, the peaks corresponding to the -LDH system (at around 431 and 508 cm^{-1}) gradually changed to the -–OOH system (at around 459 and 531 cm^{-1}) while the peaks corresponding to the B–O bond (at around 263 and 708 cm^{-1}) gradually disappeared with the application of higher oxidation potential [53–55]. *ex situ* Raman spectra of the catalyst displayed in Fig. 4e show more obvious -OOH peaks without the interference of the electrolyte liquid and the O_2 bubbles. These results indicate that the gradually formed Co-/Fe- (oxy)hydroxide, which have the optimized adsorption/desorption ability of intermediates (O*, OH*, and OOH*) [56], are the active sites of B-Co_2Fe LDH for OER. To further explore the catalytic activity of the partially amorphous B-Co_2Fe LDH under real conditions [56–58], CV curves without *iR* compensation were obtained and are shown in Fig. S20.

doi:10.1016/j.nanoen.2021.105838

Catalytic durability is another important criterion for the practical application of a catalyst. The almost overlapping polarization curves before and after 2000 cyclic voltammetry CV scans in 1 M KOH (Fig. 4f) and the well-maintained hierarchical structure after CV scanning (Fig. S21) prove that this B-Co_2Fe LDH catalyst has excellent catalytic durability and structural stability in alkaline freshwater. When cycled in 1 M KOH seawater, the resultant polarization curve shows some decline compared with the initial curve (Fig. 4f). SEM images of the post-cycling catalyst (Fig. S22) show that even though some cracks and insoluble precipitates can be observed on the macro scale, the overall hierarchical nanosheet-nanoflake structure is maintained on the micro scale, confirming the good chlorine corrosion resistance of the partially amorphous B-Co_2Fe LDH catalyst. Some common metal elements such as Mg and Ca in the natural seawater can be clearly observed in the corresponding EDS spectrum in Fig. S22e. This result reveals that even though some portions of the surface of this catalyst become covered by the precipitates, the underlying or side parts of the catalyst can remain in contact with, and react with, the electrolyte to allow the seawater electrolysis to continue. Such a hierarchical nanosheet-nanoflake structure feature, which provides large surface area to expose active sites, is more important in seawater electrolysis due to the existence of insoluble precipitates. The corresponding XPS spectra of B-Co_2Fe LDH after CV scanning (Fig. S23) show that the specific peak for B almost disappeared, indicating that boron in this case serves more as a modifier to the crystallinity of Co_2Fe LDH than to form a metallic boride catalyst (either Fe-B or Co-B). Both Co and Fe were oxidized to higher oxidation states corresponding to Co-–/Fe-–OOH, as shown by the slight shifts in their XPS spectra in Fig. S23a–b, respectively. The increased intensity of the specific peak for O in Fig. S23d proves the formation of -–OOH during CV cycling, matching the Raman result (Fig. 4e). The well-maintained hierarchical structure and the partially amorphous phase feature were also confirmed by TEM and HRTEM images obtained after CV scanning and shown in Fig. S24a–b and S24c, respectively. The durability of the B-Co_2Fe LDH catalyst was then determined by chronopotentiometric measurements performed at industrial-scale densities of 100 and 500 mA cm^{-2} in both 1 M KOH and 1 M KOH seawater electrolytes. As shown in Fig. 4g, the potential fluctuations at current densities of 100 and 500 mA cm^{-2} over 100 h continuous testing in 1 M KOH are only 22 and 37 mV, respectively. In 1 M KOH seawater (Fig. 4h), this catalyst can still work over such long-term testing with only slight increases in the potential fluctuations (46 and 65 mV for 100 and 500 mA cm^{-2}, respectively), showing great potential for practical fuel gas production from natural seawater at industrial-scale current densities. The poorer catalytic activity in seawater is mainly due to obstruction of active sites by chlorine ions and surface poisoning by insoluble precipitates, which has also been discussed in previous studies [6–8,10]. Additionally, the possible existence of hypochlorite products in the 1 M KOH seawater electrolyte after long-term stability testing was determined using a colorimetric reagent. As shown in Fig. S25, there is no color change in the reagent, indicating that no hypochlorite was formed during OER stability testing, which matches well with the GC test result shown in Fig. 4c.

A tremendous amount of research on LDH-based catalysts has been reported in the last few years, most of which has focused on doping or coupling with other compounds to enhance the catalytic performance, while structure modeling and crystallinity tuning have been less studied. Here, to overcome the drawbacks of LDH catalysts, such as poor conductivity and limited active sites, a novel and scalable strategy was developed to synthesize partially amorphous B-Co_2Fe LDH with a hierarchical nanosheet-nanoflake structure. First, the direct growth of the B-Co_2Fe LDH catalyst on conductive NF can enhance the transportation of electrons and stabilize the structure, while the hierarchical structure can provide a large surface area to rivet and disperse the active sites [59,60]. The self-supported and hydrophilic characteristics of the B-Co_2Fe LDH catalyst can provide adequate space for the diffusion of the electrolyte and accelerate the release of the bubbles, ensuring superior OER catalytic activity and long-term stability at high current density [12,46,47,59]. Second, in the modification step, $NaBH_4$ serves as both the boron source and the reduction reactant, which can not only react with the metallic cations to form metallic boride but also creates a great number of oxygen defects by extracting the oxygen and tuning the Co_2Fe LDH precursor into a partially amorphous phase [32,45,49]. Additionally, the defective interfaces located in the crystalline-amorphous phase boundaries can act as active sites while the amorphous phase can enhance the amount of adsorption sites for hydroxide. The modification by boron can also enhance the intrinsic catalytic kinetics and enlarge the ECSA of partially amorphous B-Co_2Fe LDH, which together lead to superior OER catalytic activity in both fresh water and seawater. Finally, the enhanced stability and corrosion resistance of B-Co_2Fe LDH, which result from its partial amorphousness feature, help it maintain both the hierarchical nanosheet-nanoflake structure and catalytic durability well

in the critical seawater condition [28,30].

3. Conclusions

We have successfully synthesized a partially amorphous B-Co_2Fe LDH catalyst using a two-step water bath reaction-chemical reduction approach. Its hierarchical nanosheet-nanoflake structure, along with its hydrophilic feature, help it possess abundant active sites and accelerated bubble-release ability, producing favorable synergistic effects for seawater electrolysis. It also has higher intrinsic catalytic kinetics, a larger ECSA, and an improved TOF, as compared with the Co_2Fe LDH precursor, resulting from the modification by boron. in situ Raman testing and post-OER analysis were applied to reveal its chemical and physical transformation during OER. Therefore, our work not only introduces and analyzes an OER catalyst for highly selective and stable seawater oxidation, but also provides a novel approach toward the fabrication of partially amorphous boron-modified LDH-based catalysts.

CRediT authorship contribution statement

Libo Wu: Conceptualization, Methodology, Investigation, Validation, Data curation, Formal analysis, Visualization, Writing - original draft. **Luo Yu**: Methodology, Formal analysis, Writing - review & editing. **Qiancheng Zhu:** Methodology, Data curation, Formal analysis. **Brian McElhenny:** Visualization, Formal analysis. **Fanghao Zhang:** Methodology, Formal analysis. **Chunzheng Wu** and **Xinxin Xing:** Investigation, Data curation, Formal analysis. **Jiming Bao:** Resources. **Shuo Chen:** Formal analysis, Resources, Supervision. **Zhifeng Ren:** Conceptualization, Methodology, Formal analysis, Writing - review & editing, Resources, Supervision.

Declaration of Competing Interest

The authors declare that they have no known competing financial interests or personal relationships that could have appeared to influence the work reported in this paper.

Appendix A. Supporting information

Supplementary data associated with this article can be found in the online version at doi:10.1016/j.nanoen.2021.105838.

References

[1] I. Staffell, D. Scamman, A. Velazquez Abad, P. Balcombe, P.E. Dodds, P. Ekins, N. Shah, K.R. Ward, The role of hydrogen and fuel cells in the global energy system, Energy Environ. Sci. 12 (2019) 463–491.

[2] F. Yu, L. Yu, I.K. Mishra, Y. Yu, Z.F. Ren, H.Q. Zhou, Recent developments in earth-abundant and non-noble electrocatalysts for water electrolysis, Mater. Today Phys. 7 (2018) 121–138.

[3] Y. Tan, H. Wang, P. Liu, Y. Shen, C. Cheng, A. Hirata, T. Fujita, Z. Tang, M. Chen, Versatile nanoporous bimetallic phosphides towards electrochemical water splitting, Energy Environ. Sci. 9 (2016) 2257–2261.

[4] P. Li, X. Duan, Y. Kuang, Y. Li, G. Zhang, W. Liu, X. Sun, Tuning electronic structure of NiFe layered double hydroxides with vanadium doping toward high efficient electrocatalytic water oxidation, Adv. Energy Mater. 8 (2018), 1703341.

[5] C. Huang, S. Cheng, L. Yu, W. Zhang, J. Zhou, Y. Zhang, Y. Yu, Electrolyzer with hierarchical transition metal sulfide and phosphide towards overall water splitting, Mater. Today Phys. 11 (2019), 100162.

[6] F. Dionigi, T. Reier, Z. Pawolek, M. Gliech, P. Strasser, Design criteria, operating conditions, and nickel-iron hydroxide catalyst materials for selective seawater electrolysis, ChemSusChem 9 (2016) 962–972.

[7] W. Tong, M. Forster, F. Dionigi, S. Dresp, R. Sadeghi Erami, P. Strasser, A.J. Cowan, P. Farràs, Electrolysis of low-grade and saline surface water, Nat. Energy 5 (2020) 367–377.

[8] S. Dresp, F. Dionigi, M. Klingenhof, P. Strasser, Direct electrolytic splitting of seawater: opportunities and challenges, ACS Energy Lett. 4 (2019) 933–942.

[9] L. Yu, L. Wu, B. McElhenny, S. Song, D. Luo, F. Zhang, Y. Yu, S. Chen, Z. Ren, Ultrafast room-temperature synthesis of porous S-doped Ni/Fe (oxy)hydroxide electrodes for oxygen evolution catalysis in seawater splitting, Energy Environ. Sci. 13 (2020) 3439–3446.

[10] Y. Kuang, M.J. Kenney, Y. Meng, W.-H. Hung, Y. Liu, J.E. Huang, R. Prasanna, P. Li, Y. Li, L. Wang, M.-C. Lin, M.D. McGehee, X. Sun, H. Dai, Solar-driven, highly sustained splitting of seawater into hydrogen and oxygen fuels, Proc. Natl. Acad. Sci. 116 (2019) 6624–6629.

[11] T. Hisatomi, K. Domen, Reaction systems for solar hydrogen production via water splitting with particulate semiconductor photocatalysts, Nat. Catal. 2 (2019) 387–399.

[12] X. Yu, Z.Y. Yu, X.L. Zhang, Y.R. Zheng, Y. Duan, Q. Gao, R. Wu, B. Sun, M.R. Gao, G. Wang, S.H. Yu, Superaerophobic" nickel phosphide nanoarray catalyst for efficient hydrogen evolution at ultrahigh current densities, J. Am. Chem. Soc. 141 (2019) 7537–7543.

[13] L. Wu, L. Yu, F. Zhang, B. McElhenny, D. Luo, A. Karim, S. Chen, Z. Ren, Adv. Funct. Mater. (2020), 2006484.

[14] M. Guo, L. Zhou, Y. Li, Q. Zheng, F. Xie, D. Lin, Unique nanosheet–nanowire structured CoMnFe layered triple hydroxide arrays as self-supporting electrodes for a high-efficiency oxygen evolution reaction, J. Mater. Chem. A 7 (2019) 13130–13141.

[15] L. Wu, L. Yu, X. Xiao, F. Zhang, S. Song, S. Chen, Z. Ren, Reserach 2020 (2020), 3976278.

[16] M. Gong, Y. Li, H. Wang, Y. Liang, J.Z. Wu, J. Zhou, J. Wang, T. Regier, F. Wei, H. Dai, An advanced Ni–Fe layered double hydroxide electrocatalyst for water oxidation, J. Am. Chem. Soc. 135 (2013) 8452–8455.

[17] X. Lu, C. Zhao, Electrodeposition of hierarchically structured three-dimensional nickel–iron electrodes for efficient oxygen evolution at high current densities, Nat. Commun. 6 (2015), 6616.

[18] L. Yu, H. Zhou, J. Sun, F. Qin, F. Yu, J. Bao, Y. Yu, S. Chen, Z. Ren, Cu nanowires shelled with NiFe layered double hydroxide nanosheets as bifunctional electrocatalysts for overall water splitting, Energy Environ. Sci. 10 (2017) 1820–1827.

[19] Y. Hou, M.R. Lohe, J. Zhang, S. Liu, X. Zhuang, X. Feng, Vertically oriented cobalt selenide/NiFe layered-double-hydroxide nanosheets supported on exfoliated graphene foil: an efficient 3D electrode for overall water splitting, Energy Environ. Sci. 9 (2016) 478–483.

[20] H. Zhang, X. Li, A. Hähnel, V. Naumann, C. Lin, S. Azimi, S.L. Schweizer, A. W. Maijenburg, R.B. Wehrspohn, Bifunctional heterostructure assembly of NiFe LDH nanosheets on NiCoP nanowires for highly efficient and stable overall water splitting, Adv. Funct. Mater. 28 (2018), 1706847.

[21] L. Yu, H. Zhou, J. Sun, F. Qin, D. Luo, L. Xie, F. Yu, J. Bao, Y. Li, Y. Yu, S. Chen, Z. Ren, Hierarchical Cu@CoFe layered double hydroxide core-shell nanoarchitectures as bifunctional electrocatalysts for efficient overall water splitting, Nano Energy 41 (2017) 327–336.

[22] A.-L. Wang, H. Xu, G.-R. Li, NiCoFe layered triple hydroxides with porous structures as high-performance electrocatalysts for overall water splitting, ACS Energy Lett. 1 (2016) 445–453.

[23] G. Chen, T. Wang, J. Zhang, P. Liu, H. Sun, X. Zhuang, M. Chen, X. Feng, Membranes: carbon nanotube porins in amphiphilic block copolymers as fully synthetic mimics of biological membranes (Adv. Mater. 51/2018), Adv. Mater. 30 (2018), 1870392.

[24] D. Wang, Q. Li, C. Han, Q. Lu, Z. Xing, X. Yang, Atomic and electronic modulation of self-supported nickel-vanadium layered double hydroxide to accelerate water splitting kinetics, Nat. Commun. 10 (2019), 3899.

[25] L. Lv, Z. Yang, K. Chen, C. Wang, Y. Xiong, 2D Layered double hydroxides for oxygen evolution reaction: from fundamental design to application, Adv. Energy Mater. 9 (2019), 1803358.

[26] P. Li, M. Wang, X. Duan, L. Zheng, X. Cheng, Y. Zhang, Y. Kuang, Y. Li, Q. Ma, Z. Feng, W. Liu, X. Sun, Boosting oxygen evolution of single-atomic ruthenium through electronic coupling with cobalt-iron layered double hydroxides, Nat. Commun. 10 (2019), 1711.

[27] Y. Wang, D. Yan, S. El Hankari, Y. Zou, S. Wang, Recent progress on layered double hydroxides and their derivatives for electrocatalytic water splitting, Adv. Sci. 5 (2018), 1800064.

[28] S. Yan, K.P. Abhilash, L. Tang, M. Yang, Y. Ma, Q. Xia, Q. Guo, H. Xia, Nanodrugs: supramolecular protein nanodrugs with coordination- and heating-enhanced photothermal effects for antitumor therapy (Small 52/2019), Small 15 (2019), 1970286.

[29] J. Masa, P. Weide, D. Peeters, I. Sinev, W. Xia, Z. Sun, C. Somsen, M. Muhler, W. Schuhmann, Amorphous cobalt boride (Co_2B) as a highly efficient nonprecious catalyst for electrochemical water splitting: oxygen and hydrogen evolution, Adv. Energy Mater. 6 (2016), 1502313.

[30] H. Ren, X. Sun, C. Du, J. Zhao, D. Liu, W. Fang, S. Kumar, R. Chua, S. Meng, P. Kidkhunthod, L. Song, S. Li, S. Madhavi, Q. Yan, Amorphous Fe–Ni–P–B–O nanocages as efficient electrocatalysts for oxygen evolution reaction, ACS Nano 13 (2019) 12969–12979.

[31] H. Yang, Z. Chen, P. Guo, B. Fei, R. Wu, B-doping-induced amorphization of LDH for large-current-density hydrogen evolution reaction, Appl. Catal. B Environ. 261 (2020), 118240.

[32] S. Sun, T. Zhai, C. Liang, S.V. Savilov, H. Xia, Boosted crystalline/amorphous Fe_2O_3-δ core/shell heterostructure for flexible solid-state pseudocapacitors in large scale, Nano Energy 45 (2018) 390–397.
[33] M. Fang, D. Han, W.B. Xu, Y. Shen, Y. Lu, P. Cao, S. Han, W. Xu, D. Zhu, W. Liu, J. C. Ho, Surface-guided formation of amorphous mixed-metal oxyhydroxides on ultrathin MnO_2 nanosheet arrays for efficient electrocatalytic oxygen evolution, Adv. Energy Mater. 10 (2020), 2001059.
[34] W. Cai, R. Chen, H. Yang, H.B. Tao, H.Y. Wang, J. Gao, W. Liu, S. Liu, S.F. Hung, B. Liu, Amorphous versus crystalline in water oxidation catalysis: a case study of NiFe alloy, Nano Lett. 20 (2020) 4278–4285.
[35] C. Yoon, D.L. Cocke, Potential of amorphous materials as catalysts, J. Non-Cryst. Solids 79 (1986) 217–245.
[36] Z. Dong, F. Lin, Y. Yao, L. Jiao, Crystalline $Ni(OH)_2$/amorphous NiMoOx mixed-catalyst with Pt-Like performance for hydrogen production, Adv. Energy Mater. 9 (2019), 1902703.
[37] T. ul Haq, S.A. Mansour, A. Munir, Y. Haik, Gold-supported gadolinium doped cob amorphous sheet: a new benchmark electrocatalyst for water oxidation with high turnover frequency, Adv. Funct. Mater. 30 (2020), 1910309.
[38] H. Park, E. Lee, M. Lei, H. Joo, S. Coh, B.P.T. Fokwa, Canonic-Like HER activity of Cr1–xMoxB2Solid solution: overpowering Pt/C at high current density, Adv. Mater. 32 (2020), 2000855.
[39] S. Gupta, M.K. Patel, A. Miotello, N. Patel, Metal boride-based catalysts for electrochemical water-splitting: a review, Adv. Funct. Mater. 30 (2019), 1906481.
[40] Z. Huang, S. Wang, R.D. Dewhurst, N.V. Ignat'ev, M. Finze, H. Braunschweig, Boron: its role in energy-related processes and applications, Angew. Chem. Int. Ed. 59 (2020) 8800–8816.
[41] Z. Chen, X. Duan, W. Wei, S. Wang, Z. Zhang, B.-J. Ni, Boride-based electrocatalysts: emerging candidates for water splitting, Nano Res. 13 (2020) 293–314.
[42] P. Chen, K. Xu, T. Zhou, Y. Tong, J. Wu, H. Cheng, X. Lu, H. Ding, C. Wu, Y. Xie, Strong-coupled cobalt borate nanosheets/graphene hybrid as electrocatalyst for water oxidation under both alkaline and neutral conditions, Angew. Chem., Int. Ed. 55 (2016) 2488–2492.
[43] H. Han, H. Choi, S. Mhin, Y.-R. Hong, K.M. Kim, J. Kwon, G. Ali, K.Y. Chung, M. Je, H.N. Umh, D.-H. Lim, K. Davey, S.-Z. Qiao, U. Paik, T. Song, Advantageous crystalline–amorphous phase boundary for enhanced electrochemical water oxidation, Energy Environ. Sci. 12 (2019) 2443–2454.
[44] L. Wu, L. Yu, F. Zhang, D. Wang, D. Luo, S. Song, C. Yuan, A. Karim, S. Chen, Z. Ren, Facile synthesis of nanoparticle-stacked tungsten-doped nickel iron layered double hydroxide nanosheets for boosting oxygen evolution reaction, J. Mater. Chem. A 8 (2020) 8096–8103.
[45] T. Zhai, S. Sun, X. Liu, C. Liang, G. Wang, H. Xia, Achieving insertion-like capacity at ultrahigh rate via tunable surface pseudocapacitance, Adv. Mater. 30 (2018), 1706640.
[46] Y. Luo, L. Tang, U. Khan, Q. Yu, H.M. Cheng, X. Zou, B. Liu, Morphology and surface chemistry engineering toward pH-universal catalysts for hydrogen evolution at high current density, Nat. Commun. 10 (2019), 269.
[47] C. Liang, P. Zou, A. Nairan, Y. Zhang, J. Liu, K. Liu, S. Hu, F. Kang, H.J. Fan, C. Yang, Exceptional performance of hierarchical Ni–Fe oxyhydroxide@NiFe alloy nanowire array electrocatalysts for large current density water splitting, Energy Environ. Sci. 13 (2020) 86–95.
[48] J.M.V. Nsanzimana, Y. Peng, Y.Y. Xu, L. Thia, C. Wang, B.Y. Xia, X. Wang, an efficient and earth-abundant oxygen-evolving electrocatalyst based on amorphous metal borides, Adv. Energy Mater. 8 (2018), 1701475.
[49] W.J. Jiang, S. Niu, T. Tang, Q.H. Zhang, X.Z. Liu, Y. Zhang, Y.Y. Chen, J.H. Li, L. Gu, L.J. Wan, J.S. Hu, Crystallinity-modulated electrocatalytic activity of a nickel(II) borate thin layer on Ni_3B for efficient water oxidation, Angew. Chem. Int. Ed. 56 (2017) 6572–6577.
[50] S. Jaiswar, K.D. Mandal, Evidence of enhanced oxygen vacancy defects inducing ferromagnetism in multiferroic $CaMn_7O_{12}$ manganite with sintering time, J. Phys. Chem. C 121 (2017) 19586–19601.
[51] S. Liu, J. Zhu, M. Sun, Z. Ma, K. Hu, T. Nakajima, X. Liu, P. Schmuki, L. Wang, Promoting the hydrogen evolution reaction through oxygen vacancies and phase transformation engineering on layered double hydroxide nanosheets, J. Mater. Chem. A 8 (2020) 2490–2497.
[52] C. Wu, S. Xue, Z. Qin, M. Nazari, G. Yang, S. Yue, T. Tong, H. Ghasemi, F.C. R. Hernandez, S. Xue, D. Zhang, H. Wang, Z.M. Wang, S. Pu, J. Bao, Making g-C_3N_4 ultra-thin nanosheets active for photocatalytic overall water splitting, Appl. Catal. B Environ. 282 (2021), 119557.
[53] M.W. Louie, A.T. Bell, An investigation of thin-film Ni–Fe oxide catalysts for the electrochemical evolution of oxygen, J. Am. Chem. Soc. 135 (2013) 12329–12337.
[54] J. Li, H. Chen, Y. Liu, R. Gao, X. Zou, In situstructural evolution of a nickel boride catalyst: synergistic geometric and electronic optimization for the oxygen evolution reaction, J. Mater. Chem. A 7 (2019) 5288–5294.
[55] Z. Qiu, C.-W. Tai, G.A. Niklasson, T. Edvinsson, Direct observation of active catalyst surface phases and the effect of dynamic self-optimization in NiFe-layered double hydroxides for alkaline water splitting, Energy Environ. Sci. 12 (2019) 572–581.
[56] F. Dionigi, Z. Zeng, I. Sinev, T. Merzdorf, S. Deshpande, M.B. Lopez, S. Kunze, I. Zegkinoglou, H. Sarodnik, D. Fan, A. Bergmann, J. Drnec, J.F. Araujo, M. Gliech, D. Teschner, J. Zhu, W.X. Li, J. Greeley, B.R. Cuenya, P. Strasser, In-situ structure and catalytic mechanism of NiFe and CoFe layered double hydroxides during oxygen evolution, Nat. Commun. 11 (2020), 2522.
[57] S. Anantharaj, S.R. Ede, K. Karthick, S. Sam Sankar, K. Sangeetha, P.E. Karthik, S. Kundu, Precision and correctness in the evaluation of electrocatalytic water splitting: revisiting activity parameters with a critical assessment, Energy Environ. Sci. 11 (2018) 744–771.
[58] L. Yu, Z. Ren, Systematic study of the influence of iR compensation on water electrolysis, Mater. Today Phys. 14 (2020), 100253.
[59] R. Du, X. Jin, R. Hübner, X. Fan, Y. Hu, A. Eychmüller, Engineering self-supported noble metal foams toward electrocatalysis and beyond, Adv. Energy Mater. 10 (2019), 1901945.
[60] J. Zhang, Q. Zhang, X. Feng, Support and interface effects in water-splitting electrocatalysts, Adv. Mater. 31 (2019), 1808167.

Libo Wu is currently a PhD candidate under the supervision of Prof. Ren in Department of Physics and TcSUH at University of Houston. He received his B.S. and M.S. degrees in Material Science from Jilin University and then joined Prof. Ren's group since 2018. His current research focus is discovering novel catalysts for seawater electrolysis.

Dr. Luo Yu is currently a postdoctoral fellow in Department of Physics and TcSUH at University of Houston. He received his Ph.D. degree and B.S. degree from Central China Normal University in 2018 and 2013, respectively. He joined Prof. Ren's group since 2016. His research focuses on developing efficient non-noble metal catalysts for seawater splitting and CO_2 reduction in electrocatalysis and photocatalysis.

Qiancheng Zhu received his B.S. degree in Physics and Chemistry from Central China Normal University in 2015. He is currently a Ph.D. candidate in Prof. Ying Yu's group at Central China Normal University and a Joint Ph.D. student in Prof. Ren's group at University of Houston. His research mainly focuses on designing efficient energy storage and functional materials in environmental and catalytic application.

Brian McElhenny is a graduate student in the Department of Physics at the University of Houston, where he also earned B.S. degrees in Physics and Mathematics. Joining Prof. Shuo Chen's research group in 2019 led to a focus on Transmission Electron Microscopy and collaboration with a variety of TcSUH projects. As a PhD candidate, his research focus includes in-situ TEM techniques designed to study the intergranular electric potentials within micro/nano-crystalline engineered thermoelectric materials.

Fanghao Zhang is currently a PhD candidate under the supervision of Prof. Ren in Department of Physics and TcSUH at University of Houston. He received his B.S. degree from China University of Geosciences (Wuhan) and then joined Prof. Ren's group at University of Houston since 2017. His current research direction is developing efficient non-noble metal catalysts for water and seawater electrolysis.

Dr. Chunzheng Wu is a postdoc fellow in Prof. Jiming Bao's group at the University of Houston. He received his Ph.D. degree in nanochemistry from Istituto Italiano di Tecnologia (Italy) in 2017. His research focuses on nano-synthesis and heterogeneous photo- and thermal- catalysis.

Dr. Xinxin Xing is currently a postdoc fellow in Prof. Jiming Bao's group in the Department of Electrical and Computer Engineering at the University of Houston. She received her Ph. D. degree from Yunnan University in 2019. Her current research interests focus on the synthesis and characterization of nanomaterials for high-efficient electrocatalysts and photocatalysts toward water splitting.

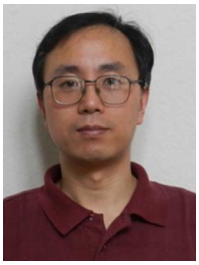

Dr. Jiming Bao is a professor of Electrical and Computer engineering at the University of Houston. He graduated from Zhejiang University with B.S. and M.S. in physics in 1992 and 1995, respectively. He obtained his Ph.D. in applied physics in 2003 from the University of Michigan, he then did postdoctoral research at Harvard University before joining the University of Houston in 2008 as an assistant professor. His current research covers many interdisciplinary topics ranging from solar energy conversion to fiber optic sensing. More information can be found from Dr. Bao's group website at http://nano.ee.uh.edu/.

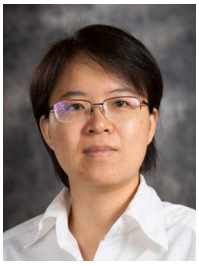

Dr. Shuo Chen is currently an associate professor in Department of Physics at the University of Houston. She obtained her B. S. degree in Physics from Peking University in China in 2002 and then Ph.D. degree in Physics from Boston College in 2006. From 2006–2011, she was a postdoctoral associate in the Department of Mechanical Engineering at MIT. Her research focuses on materials physics, especially synthesis and in situ electron microscopy of nanostructured materials for energy conversion and storage, such as thermoelectric materials, electrocatalysts, and batteries.

Dr. Zhifeng Ren is currently M.D. Anderson Chair Professor in the Department of Physics at the University of Houston, Director of the Texas Center for Superconductivity at the University of Houston (TcSUH), and Editor-in-Chief of *Materials Today Physics*. He obtained his Ph.D. degree from the Institute of Physics of the Chinese Academy of Sciences in China in 1990. He was a postdoctoral fellow and research faculty member at SUNY Buffalo (1990–1999) before joining Boston College as an Associate Professor in 1999. He specializes in thermoelectric materials, carbon nanotubes and semiconducting nanostructures, non-noble-metal catalysts for water splitting, flexible transparent conductors, etc.